Rare Metal Materials and Engineering
Volume 48, Issue 1, January 2019
Available online at www.rmme.ac.cn

Science Press

Cite this article as: Rare Metal Materials and Engineering, 2019, 48(1): 0009-0015.

ARTICLE

In situ Synthesis of Nano-WO_3 Particles Attached to Sphere-like Micro-WO_3 Using Jagged CNTs as Template

Yin Yanhong[1, 2], **Tong Zhen**[1], **Xing Kangqian**[1], **Wu Ziping**[1, 2], **Li Yesheng**[1], **Liu Xianbin**[1], **Liang Tongxiang**[1], **Liao Chunfa**[1], **Jiang Longke**[1], **Shao Jianfeng**[1]

[1] School of Materials Science and Engineering, Jiangxi University of Science and Technology, Ganzhou 341000, China; [2] Engineering Research Center of High-efficiency Development and Application Technology of Tungsten Resources (Ministry of Education) , Ganzhou 341000, China

Abstract: The CNT bundles can be jagged and used as a template to load the precursor H_2WO_4. The H_2WO_4 seeds can be enclosed by the jagged CNT template during liquid precipitation. The H_2WO_4 clusters with an average size of 500 nm consist of nanosized H_2WO_4 with 10~20 nm in diameter, which display a high specific surface area of 85.24 $m^2 \cdot g^{-1}$ and a total pore volume of 0.2933 $m^3 \cdot g^{-1}$. After thermal treating of H_2WO_4/CNTs under an oxygen atmosphere, nano-WO_3 particles attached to the sphere-like micro-WO_3 can be easily obtained by removing the CNT template. Its specific surface area and total pore volume are 18.7 $m^2 \cdot g^{-1}$ and 0.2055 $m^3 \cdot g^{-1}$, respectively. These results indicate that the jagged CNTs can play an important role for effective mediating WO_3 with a hierarchical size, and exhibit excellent prospects for preparing micro-nanostructured materials.

Key words: sphere-like; WO_3; jagged; CNT; template

Micro/nano-structured tungsten oxide (WO_3) consisting of sheet, rod, or sphere morphology has received increasing attentions[1-3], which is mainly due to its potential for broad applications, such as catalysts, electrochromic devices or gas sensors[4-6]. A variety of methods[7-10] such as reactive vapor transport method, template method and soft chemical synthesis method, are used to design micro/nano-WO_3 with a specific morphology. However, the morphology and size of WO_3 is mainly affected by the precursor H_2WO_4 during liquid synthesis process [11-14], therefore, it is crucial to mediate the morphology and size of the precursor H_2WO_4.

Carbon nanotubes (CNTs) with a typical one-dimensional (1D) structure are ideal for the preparation of limited types of highly dispersive nanomaterials with a high specific surface area [15-18]. The CNTs bundles are usually used as templates to mediate the morphology, size and structure of the target materials [19-22]. Meanwhile, the outer surface of the CNTs is usually functionalized using strong acid (such as concentrated nitric acid) by the introduction many active groups. Therefore, the prepared micro/nanostructured materials usually grow at active locations on the surface of the CNTs, and ultimately exhibit particle, rod and wire morphologies[23-26]. However, sphere-like micromaterials composed of nanoparticles are seldom prepared by CNTs as a template. The CNT bundles with targeted modifications are benificial for obtaining specific materials with special morphology[27-30].

It is found that the CNT bundles can be effectively jagged by solid-phase redox (as shown in Experimental Section 1.1). The highly dispersed CNT bundles with jagged edges can be used as a template to enclose the precursor H_2WO_4 in the liquid reaction process. The jagged CNT bundles can effectively mediate the morphology and size of WO_3, and exhibit excellent prospects for preparation of sphere-like micro-nanostructured materials.

1 Experiment

1.1 Preparation and dispersion of the jagged CNT template

Received date: January 25, 2018
Foundation item: National Natural Science Foundation of China (51202095, 51264010); the Department of Science & Technology of Jiangxi Province (GJJ160604, 20122BAB216013, 20121BBE50027, 20153BCB23011, 20133BBE50005, 20142BDH80025); the Program for Excellent Young Talents, JXUST

Corresponding author: Wu Ziping, Ph. D., Associate Professor, School of Materials Science and Engineering, Jiangxi University of Science and Technology, Ganzhou 341000, P. R. China, Tel: 0086-797-8312422, E-mail: wuziping724@jxust.edu.cn

The CNTs can be prepared by an approach reported [31] in our precious studies (as shown in Fig. 1a and 1b). Herein, the CNTs are jagged using asolid -phase redox reaction as follows: Firstly, iron (III) oxide-hydroxide is deposited on the surfaces of CNT bundles (as shown in Fig. 1a and 1b) by liquid deposition method. Then the CNTs/iron (III) oxide-hydroxide is placed in the tubular furnace and then heated to 850 °C under nitrogen atmosphere, and the iron oxide particles are reduced by graphitic carbon. The jagged CNTs can be achieved by this localized reaction with the consumption of graphitic carbon. Finally, the iron oxide particles generated from the above reaction are removed using dilute hydrochloric acid. The jagged CNT bundles can be obtained (as shown in Fig. 1c). After the above cutting process, the jagged CNTs are dispersed in ethylene glycol (EG)[32], the CNTs/EG suspension (noted as suspension A) can be obtained.

1.2 Synthesis and dehydration of tungsten acid/CNTs

Ammonium paratungstate (APT) is dissolved in ammonia by heating, named as solution B. The above suspension A is slowly added to solution B with stirring persistently. Then, the hydrochloric acid is added dropwise to the above system and heated to 140 °C for 4 h, where, the jagged CNTs are used as template for supporting tungsten acid. When cooled to room temperature, the as-prepared sample is filtered and washed repeatedly with excess deionized water and ethanol. The dark green product (CNTs/H_2WO_4) can be obtained after being dried in a low-vacuum system at room temperature. The yellow ultimate product (WO_3) can be obtained after the CNTs/H_2WO_4 is calcined in an oxygen atmosphere at 600 °C for 1 h. Here oxygen atmosphere is used for removing the jagged CNT template.

1.3 Materials characterization

The phase constitution of the sample is analyzed by X-ray diffraction (XRD) analysis (Thermo ARL SCINTAG X’TRA XRD) by Cu Kα (0.1541 nm) radiation. The detailed micro morphology of the samples is characterized by transmission electron microscopy (TEM) and high-resolution transmission electron microscopy (HRTEM), using a Tecnai G2 F30 S-Twin equipped with a high-resolution digital camera and energy-dispersive full range X-ray (EDS) microanalysis system. An N_2 adsorption/desorption isotherm is obtained at the liquid nitrogen temperature using an automatic analyzer (BELSORP-miniⅡ, BEL Co., Japan). The Brunauer-Emmett-Teller (BET) surface area of the sample is obtained from the N_2 adsorption/desorption isotherms using an absorption temperature of 77 K, and the corresponding pore size distribution is calculated from a desorption branch of N_2 isotherms using the Barrett-Joyner-Halenda (BJH) method. Prior to adsorption, the sample is outgassed for 8 h under vacuum at 400 °C.

2 Results and Discussion

The detailed morphologies of the as-prepared CNTs before and after jagging were investigated by TEM (Fig. 1). The morphologies of CNTs with ferrous particles attached are shown in Fig. 1a. The CNT bundles, with diameters ranging from 5 nm to 50 nm, stick to each other because of large van der Waals forces. There are many particles attached to the surface of CNT bundles, which is confirmed by EDS in Fig. 1b. Results show that the selected area is composed of C and Fe elements with minor Cu from Cu grid of TEM. The jagged CNT bundles highly entangle with each other and have widths of approximately 30~50 nm (Fig. 1c). There are no ferrous particles attached on the surface of the CNT bundles. The edges of the CNT bundles are jagged after removing ferrous particles, which is mainly ascribed to the fact ferric oxide consuming certain carbon at 850 °C in an atmosphere of nitrogen.

The phase composition and crystallinity of the precursor and its dehydrating product are shown in Fig. 2. The phase

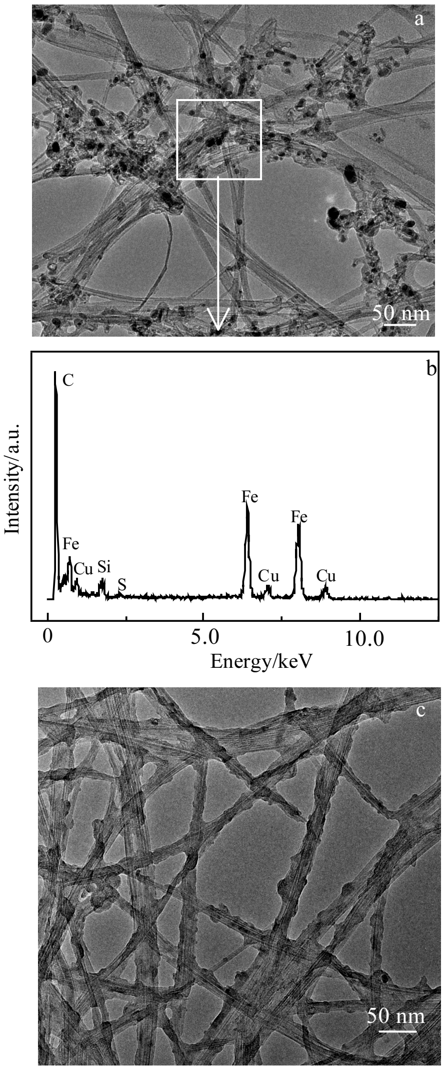

Fig. 1 Typical TEM images and EDS spectrum of CNT bundles before jagging (a, b) and after (c) jagging

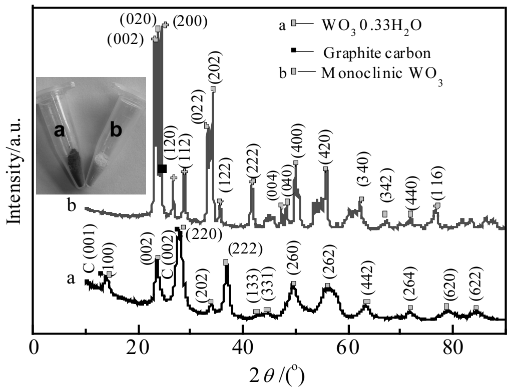

Fig. 2 XRD patterns of the precursor (a) and its dehydrating product (b) after heated to 600 °C under oxygen atmosphere

composition of the precursor before calcination is shown in the pattern a of Fig. 2. The diffraction peaks at 13.9° and 26.0° are the characteristic planes of graphite carbon of (001) and (002), respectively. And the classic diffraction peaks at 23.1°, 28.1°, 50.2°, 49.5° and 56.0° are the characteristic planes of the (002), (220), (222), (260) and (262) for $WO_3{\cdot}0.33H_2O$ (PDF# 72-0199), respectively. Therefore, the precursor can be inferred as CNTs/H_2WO_4. The evident characteristic peaks at 23.1°, 23.6° and 24.3° are also observed (pattern b in Fig. 2), which are indexed as (002), (020) and (200) planes of monoclinic WO_3 (PDF# 72-1465), respectively.

Fig. 3a shows a typical SEM image of H_2WO_4 decorated by CNTs with a diameter of approximately 500 nm. As shown in Fig. 3b (magnification of Fig. 3a), the CNT bundles located outside of the H_2WO_4 are easily observed. These results show that more mobile storage space can be provided for the H_2WO_4 particles by the interconnected jagged CNT network. The jagged CNTs existing in the reaction system not only mediate the morphology of H_2WO_4, but also control the size of H_2WO_4. The entangled jagged CNT bundles with H_2WO_4 attached can form a three-dimensional network structure. Fig. 3c shows the morphology of WO_3, which is obtained from the H_2WO_4/CNTs hybrids calcined in an oxygen atmosphere at 600 °C for the removal of the CNT template. WO_3 with a sphere-like morphology can be found. It has diameters is 0.5~1 μm. The typical HRTEM image (Fig. 3d) shows that the sphere-like micro-WO_3 is mainly composed of highly dispersed WO_3 nano-particles. We believe that the morphology and size of WO_3 are significantly influenced by those of the jagged CNT template. Many more active edges (generated by the jagged CNT bundles) in the reaction system become available from the jagged network, with a large specific surface area and space structure, which is essential for obtaining sphere-like materials.

Typical morphologies of the prepared H_2WO_4/CNTs hybrids are shown in Fig. 4a (affirmed by Fig. 2a). H_2WO_4/CNTs with diameters of 0.5 μm to 1 μm present a highly dispersive cluster-like morphology. From Fig. 4b (partial magnification of Fig. 4a), the H_2WO_4/CNTs clusters with an average size of 600 nm to 800 nm can be clearly observed. The H_2WO_4/CNTs clusters consist of H_2WO_4 seeds with a small size of approximately 10 nm (as shown in Fig. 4c), thereby indicating that high storage degree of H_2WO_4 often occurs in the three-dimentional network space of the jagged CNT bundles. The CNT bundles with jagged edges of 10~50 nm diameter further hinder the development of H_2WO_4

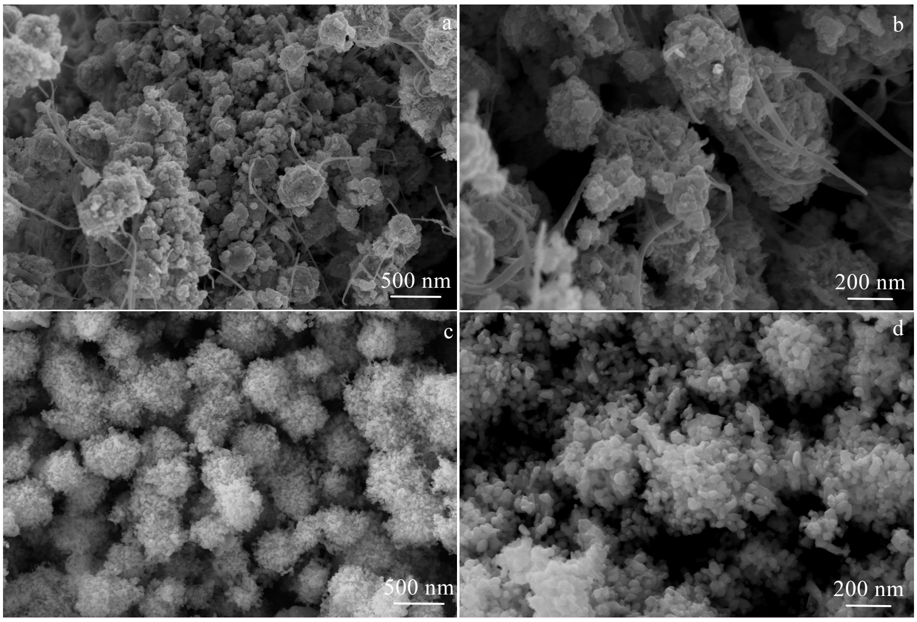

Fig. 3 Typical SEM images of as-prepared H_2WO_4/CNTs (a, b) and WO_3 (c, d)

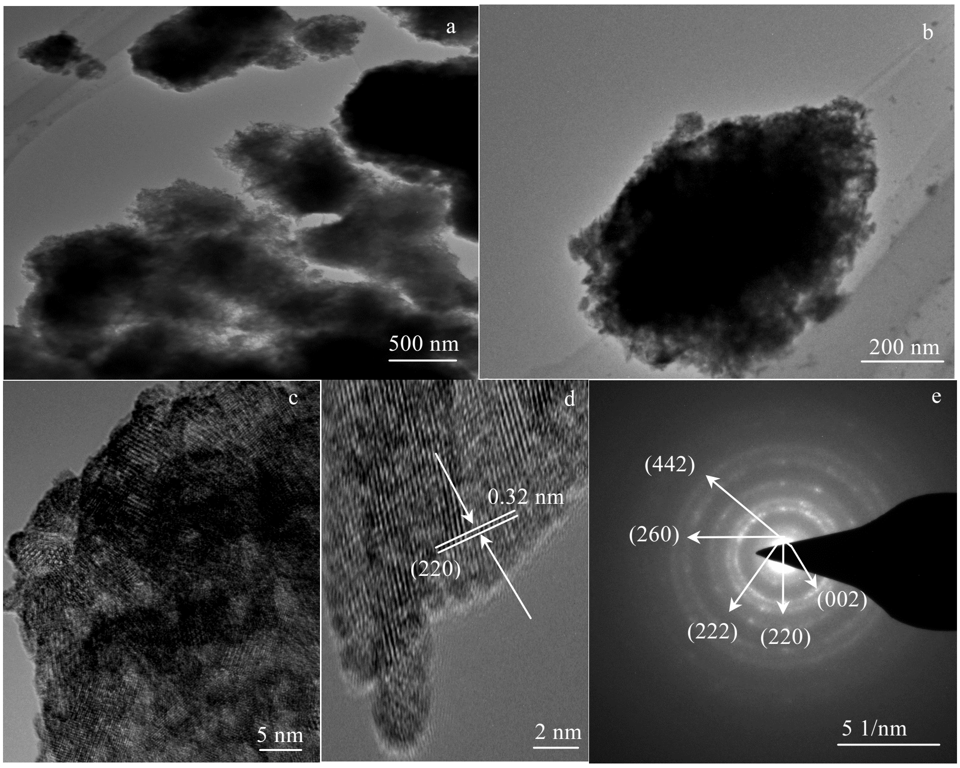

Fig.4 Typical TEM (a, b), HRTEM (c, d) images and SAED pattern (e) of H_2WO_4/CNTs

particles in the reaction process, and ensure the morphology and size of the H_2WO_4/CNTs hybrid be effectively mediated. The HRTEM image of H_2WO_4/CNTs is presented in Fig.4d. The lattice fridge with a *d*-spacing of 0.32 nm corresponds to (220) interplanar distances of $WO_3 \cdot 0.33H_2O$ (PDF# 72-0199). Based on the selected area electron diffraction (SAED) observation (Fig.4d), it can be concluded that d=0.40, 0.31, 0.236, 0.18, 0.136 nm correspond to the characteristic planes of (002), (220), (222), (260), (442) direction, respectively, which is consistent with those patterns observed in Fig.2.

Fig.5a shows the morphology of the product of WO_3. It has diameters of 200 nm to 300 nm and is composed of some dispersed particles. The CNT template is removed by calcination process in oxygen atmosphere, as confirmed by EDS in Fig.5b, which indicates that the product is composed of W and O elements with minor Cu from Cu grid of TEM. From Fig.5c, WO_3 clusters with 300 nm diameter consisted of WO_3 nano-particles, and the nano-WO_3 is well faced with diameters of 20~30 nm (Fig.5d). Based on HRTEM observation (Fig.5e), the lattice spacing of 0.38 and 0.36 nm corresponds to (002) and (200) interplanar distance of WO_3 monoclinic phase WO_3 (PDF# 72-1465), respectively. Based on the SAED observation (Fig. 5f), the particles grow along the (002) and (200) directions, which corresponds to pattern b of Fig.2.

Fig.6a shows the N_2 adsorption-desorption isotherm and pore size distribution curves. Both of H_2WO_4/CNTs (curve 1 in Fig.6a) and WO_3 (curve 2 in Fig.6a) show a certain nitrogen absorption at the low pressure region (relative pressure of 0~0.35). The adsorption capacity of H_2WO_4/CNTs (curve 1 in Fig.6a) is larger than that of WO_3 (curve 2 in Fig.6a), and the specific surface areas of H_2WO_4/CNTs and WO_3 calculated by the BET method are 85.2 and 18.7 $m^2 \cdot g^{-1}$, respectively. Calculated from the typical N_2 desorption isotherms using the BJH method, the mesoporous diameter distribution curves [33] for H_2WO_4/CNTs (curve 1) and WO_3 (curve 2) are showed in Fig.6b. The corresponding total pore volumes are 0.2933 and 0.2055 $m^3 \cdot g^{-1}$ (P/P_0=0.966), respectively, suggesting a certain decrease in surface area and pore volume of WO_3 compared with those of H_2WO_4/CNTs. H_2WO_4/CNTs (curve 1 in Fig.6b) possesses a higher specific surface area and pore volume (0~25 nm of pore radius) than those of WO_3 (curve 2 in Fig.6b), which is mainly attributed to the jagged CNTs and highly dispersed H_2WO_4 particles. The jagged CNTs efficiently prevent the aggregation of H_2WO_4 and improve its surface area and pore volume, therefore the cluster-like framework of H_2WO_4/CNTs is stabilized[34]. After removing the jagged CNT template, the pore-size distribution peak intensity of WO_3 shows a downtrend, which ascribes to the disappearance of CNTs and the partial shrinkage and collapse of the structure of WO_3 particles.

The formation process of sphere-like WO_3 is expressed in Fig.7. The introduction of the jagged CNTs is important for the morphology and size of H_2WO_4 and WO_3 in this study.

The dissolution of APT in ammonia can be expressed by the following equations:

$$5(NH_4)_2\cdot 12WO_3\cdot 5H_2O \rightarrow 10NH_4^{+} + H_2W_{12}O_{42}^{10-} + 4H_2O \quad (1)$$

$$H_2W_{12}O_{42}^{10-} \rightarrow 2HW_6O_{21}^{5-} \quad (2)$$

$$HW_6O_{21}^{5-} + 7NH_3 + 3H_2O \rightarrow 6WO_4^{2-} + 7NH_4^{+} \quad (3)$$

The balance reaction of ammonia can be showed as the following equation:

$$NH_3 + H_2O \leftrightarrow N_3H\cdot H_2O \leftrightarrow NH_4^{+} + OH^{-} \quad (4)$$

During the liquid chemical reaction, the numerous jagged CNT bundles with jagged edges display high specific surface area and Van der Waals force [35], which are easily involved with each other and further form network space structure. The main ions of NH_4^{+} and WO_4^{2-} (Eq.(3)) are easily shuttled among the network gaps or absorbed on the surface of the jagged CNT bundles. As the hydrochloric acid is added dropwise to the above alkaline system, and H^{+} firstly reacts with OH^{-}, the balance reaction of ammonia (Eq.(4)) is broken.

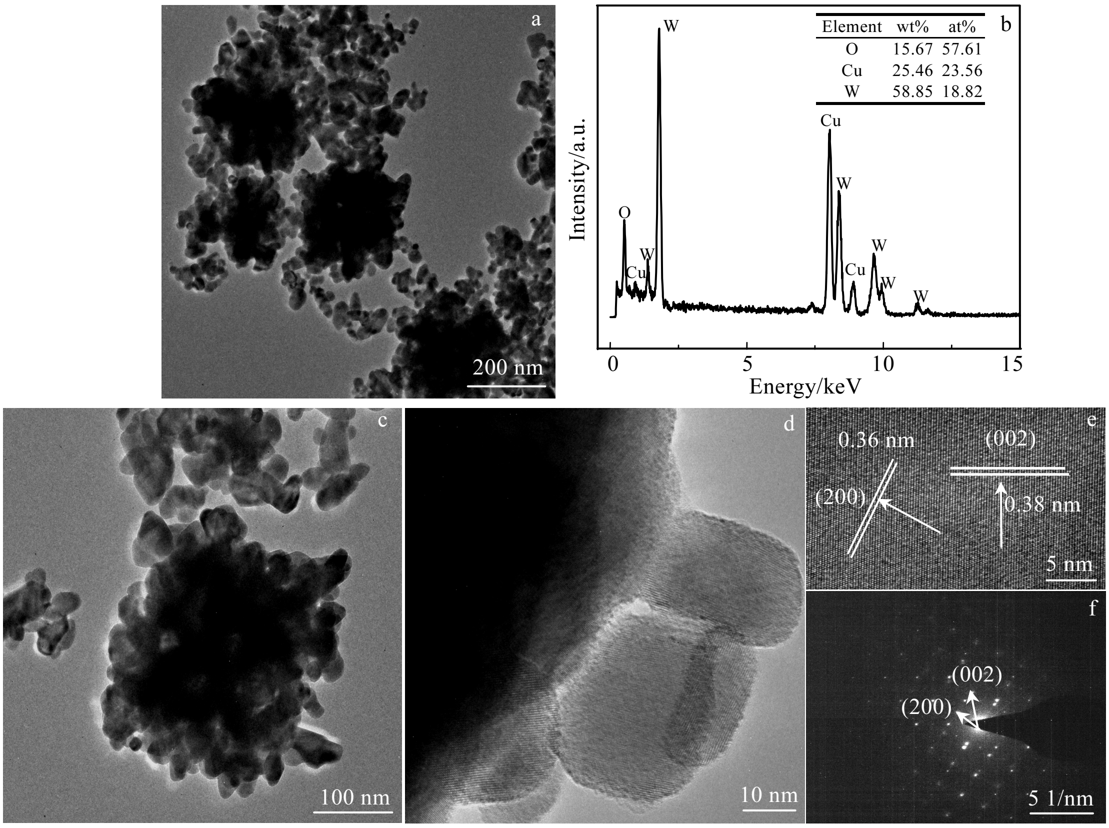

Element	wt%	at%
O	15.67	57.61
Cu	25.46	23.56
W	58.85	18.82

Fig.5 Typical TEM images (a, c, d), EDS spectra (b), HRTEM image (e) and SAED pattern (f) of WO_3 after removing CNTs

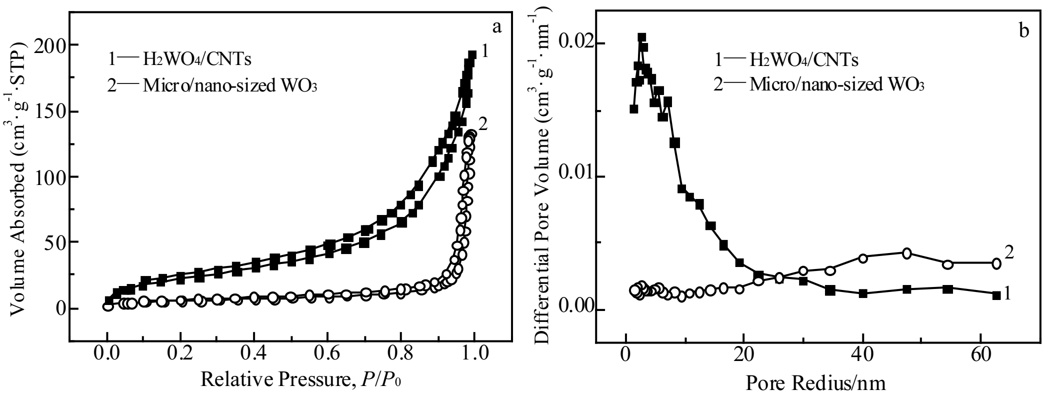

Fig.6 N_2 adsorption/desorption isotherms (a) and pore radius distributions (b) of H_2WO_4/CNTs and micro/nano-sized WO_3

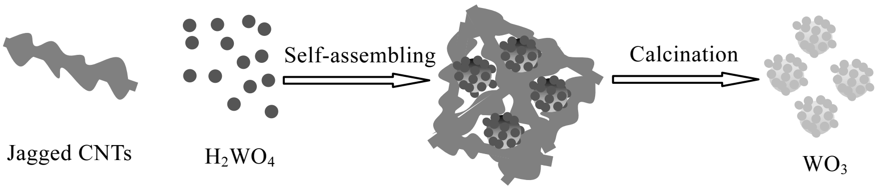

Fig. 7 Schematic illustration of H_2WO_4 self-assembled on the jagged CNT template and transformed to sphere-like micro/nano WO_3

H^+ then displaces NH_4^+ and reacts slowly with WO_4^{2-}, and the network gaps of the jagged CNT bundles can be easily occupied by H_2WO_4 colloid. The amorphous H_2WO_4 ($WO_3{\cdot}xH_2O$) colloid will transform into a stable crystalline state under the thermalchemical conditions. In addition, the prepared H_2WO_4 colloid, before being enclosed by the jagged CNT bundles, can be isolated by the jagged edges of CNT bundles in the reaction system. Consequently, the H_2WO_4 nanoparticles are loaded on the network of jagged CNT bundles and attached together. The H_2WO_4 with a cluster appearance can be produced when three-dimentional network space of the jagged CNT bundles is completely occupied by H_2WO_4. If the CNTs are not jagged in reaction solution, the prepared H_2WO_4 with a rod-like morphology can be prepared (the results are not shown). Cl^- will naturally remain together with NH_4^+ as a salt (NH_4Cl) solution, which can be removed through multiple filtering.

From Fig. 7, the CNT template with jagged edges can enable the formation of sphere-like WO_3. The sphere-like microsized WO_3 composed of nanosized WO_3 particles can be prepared. The morphology and size of WO_3 can be effectively mediated by the jagged CNTs.

3 Conclusions

1) The network CNT bundles are jagged and used as a template, and the H_2WO_4 clusters can be enclosed by the network of jagged CNT bundles in the reaction system.

2) The H_2WO_4/CNTs hybrid with a high specific surface area (SSA) of 85.24 $m^2{\cdot}g^{-1}$ and total pore volumes of 0.2933 $m^3{\cdot}g^{-1}$ can be realized. After removing the jagged CNTs, the sphere-like micro-WO_3 consisted of nano-WO_3 particles, with SSA of 18.7 $m^2{\cdot}g^{-1}$ and total pore volumes of 0.2055 $m^3{\cdot}g^{-1}$, can be successfully obtained.

3) The presence of the jagged CNTs can effectively mediate the WO_3 with a hierarchical size, and exhibits excellent prospects for preparing micro-nanostructured materials.

References

1 Weng B, Wu J, Zhang N *et al. Langmuir*[J], 2014, 30(19): 5574

2 Sun W, Yeung M T, Lech A T *et al. Nano letters*[J], 2015, 15(7): 4834

3 Yan J, Wang T, Wu G *et al. Advanced Materials*[J], 2015, 27(9): 1580

4 Bignozzi C A, Caramori S, Cristino V *et al. Chemical Society Reviews*[J], 2013, 42(6): 2228

5 Lu N, Gao X Q, Yang C *et al. Sensors and Actuators B: Chemical*[J], 2016, 223: 743

6 Zeng W, Li Y Q, Miao B *et al. Physica E*[J], 2014, 56: 1

7 Lian C, Xiao X, Chen Z *et al. Nano Research*[J], 2016, 9(2): 435

8 Bai S, Zhang K, Wang L *et al. Journal of Materials Chemistry A* [J], 2014, 2(21): 7927

9 Chiarello G L, Bernareggi M, Pedroni M *et al. Journal of Materials Chemistry A*[J], 2017(5): 12 977

10 Johansson M B, Mattsson A, Lindaquist S E *et al. Journal of Physical Chemistry C*[J], 2017, 121(135): 7412

11 Yun Y, Araujo J R, Melaet G *et al. Catalysis Letters*[J], 2017, 147(3): 622

12 Zhang H L, Yang J Q, Li D *et al. Applied Surface Science*[J], 2014, 305: 274

13 Bai S L, Zhang K W, Shu X *et al. Crystengcomm*[J], 2014, 16 (44): 10 210

14 Long H W, Zeng W, Xu S B *et al. Journal of Materials Science* [J], 2014, 25(11): 5158

15 De Volder M F, Tawfick S H, Baughman R H *et al. Science*[J], 2013, 339(6119): 535

16 Mittal G, Dhand V, Rhee K Y *et al. Journal of Industrial and Engineering Chemistry*[J], 2015, 21: 11

17 Cao Q, Han S J, Tulevski G S *et al. Nature Nanotechnology*[J], 2013, 8(3): 180

18 Wu Z P, Xu Q F, Wang J N. *Journal of Materials Science and Technology*[J], 2010, 26: 20

19 Choi S J, Kim S J, Koo W T *et al. Chemical Communications*[J], 2015, 51(13): 2609

20 Yin Y H, Ma C A, Wu Z P *et al. Journal of Materials Science and Technology*[J], 2015, 31: 888

21 Kumar R D, Andou Y, Karuppuchamy S. *Journal of Materials Science: Materials in Electronics*[J], 2017, 28(7): 5425

22 Wu Z P, Huang X L, Yin Y H *et al. Rare Metal Materials and Engineering* [J], 2014, 43(3): 535

23 Van Duy N, Hoa N D, Dat N T *et al. Science of Advanced Materials*[J], 2016, 8(3): 524

24 Wu Z P, Zhao M, Hu J W *et al. RSC Advances*[J], 2014, 4: 47414

25 Yin Y H, Ma C A, Wu Z P *et al. Rare Metals*[J], 2015(1): 1

26 Yan Y, Zhang L, Qi X Y *et al. Small* [J], 2012, 8(21): 3350

27 Ko H, Park S, Park S *et al. Journal of Nanoscience and Nanotechnology*[J], 2015, 15(7): 5295

28 Zhang Y, Jia G, Wang H. *et al. Materials Chemistry Frontiers*[J], 2017, 1(4): 709

29 Salama E I, Abbas A, Esawi A M K. *Composites Part A: Applied Science and Manufacturing* [J], 2017, 99: 84

30 Wu Z P, Zhang W B, Yin Y H *et al. Rare Metal Materials and Engineering*[J], 2015, 44: 1351

31 Wu Z P, Wang J N, Ma J. *Carbon*[J], 2008, 47: 324

32 Wu Z P, Xia B Y, Wang X X *et al. Journal of Power Sources*[J], 2010, 195: 2143

33 Khosrozadeh A, Hajabasi M A. *Applied Mathematical Modelling*[J], 2012, 36(3): 997

34 Ma J M, Zhang J, Wang S R *et al. The Journal of Physical Chemistry C* [J], 2011, 115(37): 18 157

35 Barrett E P, Joyner L G, Halenda P P. *Journal of the American Chemical society* [J], 1951,73: 373

以锯齿状碳纳米管为模板原位合成微/纳米球状氧化钨

尹艳红 [1,2]，童 珍 [1]，幸康虔 [1]，吴子平 [1,2]，黎业生 [1]，刘先斌 [1]，梁同祥 [1]，廖春发 [1]，蒋隆科 [1]，邵健锋 [1]

(1. 江西理工大学 材料科学与工程学院，江西 赣州 341000)

(2. 钨资源高效开发与应用技术工程研究中心 (教育部)，江西 赣州 341000)

摘　要：以锯齿状 CNTs 管束作为模板担载 H_2WO_4 前驱体。在液相沉积过程中 H_2WO_4 被锯齿状 CNTs 包裹，所得 H_2WO_4/CNTs 团簇的平均尺寸为 500 nm，由直径 10~20 nm 的 H_2WO_4 组成，比表面积和孔容分别为 85.24 $m^2 \cdot g^{-1}$ 和 0.2933 $m^3 \cdot g^{-1}$。将 H_2WO_4/CNTs 置于氧气气氛中进行热处理，除去 CNTs 后，得到了由纳米颗粒组成的 WO_3 微米球，比表面积和孔容分别为 18.7 $m^2 \cdot g^{-1}$ 和 0.2055 $m^3 \cdot g^{-1}$。结果表明，锯齿状 CNTs 对有效调节分层结构 WO_3 发挥重要作用，对制备微纳米结构材料具有广阔的应用前景。

关键词：球状；氧化钨；锯齿状；碳纳米管；模板

作者简介：尹艳红，女，1979 年生，博士，副教授，江西理工大学材料科学与工程学院, 江西 赣州 341000，电话：0797-8312422，E-mail: yyh79yy@163.com